

On Writing an MS Thesis

Second Line of Title if Necessary

Three Line Limit

Jae Hun Lee

A thesis submitted to the faculty of  
Brigham Young University  
in partial fulfillment of the requirements for the degree of

Master of Science

Brent E. Nelson, Chair  
Aaron R. Hawkins  
Brian A. Mazzeo

Department of Electrical and Computer Engineering  
Brigham Young University

Copyright © 2017 Jae Hun Lee  
All Rights Reserved

## ABSTRACT

On Writing an MS Thesis  
Second Line of Title if Necessary  
Three Line Limit

Jae Hun Lee  
Department of Electrical and Computer Engineering, BYU  
Master of Science

The abstract is a summary of the dissertation, thesis, or selected project with emphasis on the findings of the study. The abstract must not exceed 1 page in length. It should be printed in the same font and size as the rest of the work. The abstract precedes the acknowledgments page and the body of the work.

Keywords: thesis template, dissertation template, technical writing

## ACKNOWLEDGMENTS

Students may use the acknowledgments page to express appreciation for the committee members, friends, or family who provided assistance in research, writing, or technical aspects of the dissertation, thesis, or selected project. Acknowledgments should be simple and in good taste.

## TABLE OF CONTENTS

<b>List of Tables</b> . . . . .	<b>vi</b>
<b>List of Figures</b> . . . . .	<b>vii</b>
<b>Chapter 1 Introduction</b> . . . . .	<b>1</b>
1.1 First Section . . . . .	1
1.1.1 First Subsection . . . . .	1
1.1.2 Second Subsection . . . . .	1
1.2 Citation Example . . . . .	1
1.3 Fixed Width Figure Example . . . . .	1
1.4 Math and Equation Example, Where the Heading Is Made so Long That It Extends onto a Second Line . . . . .	2
<b>Chapter 2 Gimbal Control</b> . . . . .	<b>4</b>
2.1 Angle Commanding Gimbal Control . . . . .	4
2.1.1 Coordinate Frame Convention and Projective Camera Geometry . . . . .	4
2.1.2 Derivation . . . . .	7
2.1.3 Hardware Testing Result . . . . .	8
2.2 Angular Velocity Commanding Gimbal Control . . . . .	9
2.2.1 Image Jacobian . . . . .	9
2.2.2 Feedback Linearization-based Visual Pointing and Tracking . . . . .	11
<b>Chapter 3 UAV Control</b> . . . . .	<b>17</b>
3.1 UAV visual-servoing controller using projective camera geometry . . . . .	17
3.1.1 Coordinate Frame Convention . . . . .	17
3.1.2 Forward and heading motion control . . . . .	18
<b>Chapter 4 Advanced UAV Control</b> . . . . .	<b>21</b>
4.1 Motivation . . . . .	21
4.2 Controller Derivation for Simple UAV dynamics . . . . .	22
<b>References</b> . . . . .	<b>29</b>
<b>Appendix A Making a Figure with Width Based on Page Size</b> . . . . .	<b>30</b>
A.1 Width Based on Page Size Figure Example . . . . .	30
<b>Appendix B Formatting Guidelines for Thesis</b> . . . . .	<b>31</b>
B.1 Font . . . . .	31
B.2 Margins . . . . .	31
B.3 Printing . . . . .	31
B.4 Page Numbering . . . . .	31
B.5 Spacing . . . . .	32

<b>B.6 Figures</b>	33
<b>B.7 Tables</b>	33

## LIST OF TABLES

## LIST OF FIGURES

1.1	Example small width figure	2
1.2	Example fixed width figure	2
2.1	Frames of interest: body frame, gimbal-1 frame, and gimbal frame	5
2.2	Camera frame and visual aid for projective camera model	6
2.3	Prototype hardware to test gimbal control algorithm	9
2.4	Hardware demonstration. The gimbal control algorithm is keeping the target object at the center of the camera field of view.	15
2.5	Elevation and cross-elevation axis	16
2.6	Angular velocity commanding gimbal controller block diagram	16
3.1	Side view of the multirotor.	18
4.1	Non-flat-earth model example. The unit optical axis vector $\hat{m}$ and the unit line of sight vector $\hat{l}$ are key components of the controller presented in this chapter.	21
4.2	Graphical overview of the problem	22
4.3	Projection onto the null space of the optical axis unit vector	23
4.4	Simple UAV dynamics visual servoing Simulink simulation. The blue square is flying UAV at constant altitude and the red square is a target on the ground moving at 5m/s	28
4.5	The horizontal error between the unit LOS vector and the unit optical axis vector converges to zero.	28
A.1	Example figure whose width depends on page size	30

## CHAPTER 1. INTRODUCTION

This is an example of the introduction. It's pretty simple and shows off some of the basic commands.

### 1.1 First Section

This part shows how you can divide things into sections.

#### 1.1.1 First Subsection

Also into subsections.

#### 1.1.2 Second Subsection

Which really helps organization and automatically gets added to the Table of Contents and gets linked to by the hyperref package.

### 1.2 Citation Example

One of the greatest parts about L<sup>A</sup>T<sub>E</sub>X is BibTeX. You can just call the \cite command and it will organize the whole references section for you as long as there is an entry in the refs.bib file (or whichever other .bib file you tell it to use; see the source for master.tex). Here is an example of citing previousworks [?], [?].

### 1.3 Fixed Width Figure Example

This part also shows how to include a basic figure like the ones shown in Figures 1.1 and 1.2.

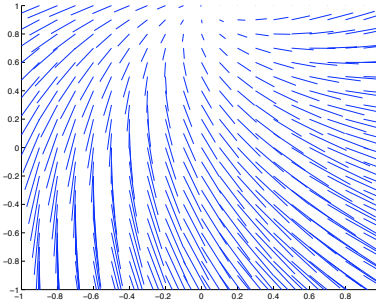


Figure 1.1: Example small width figure, showing how to use the width option.

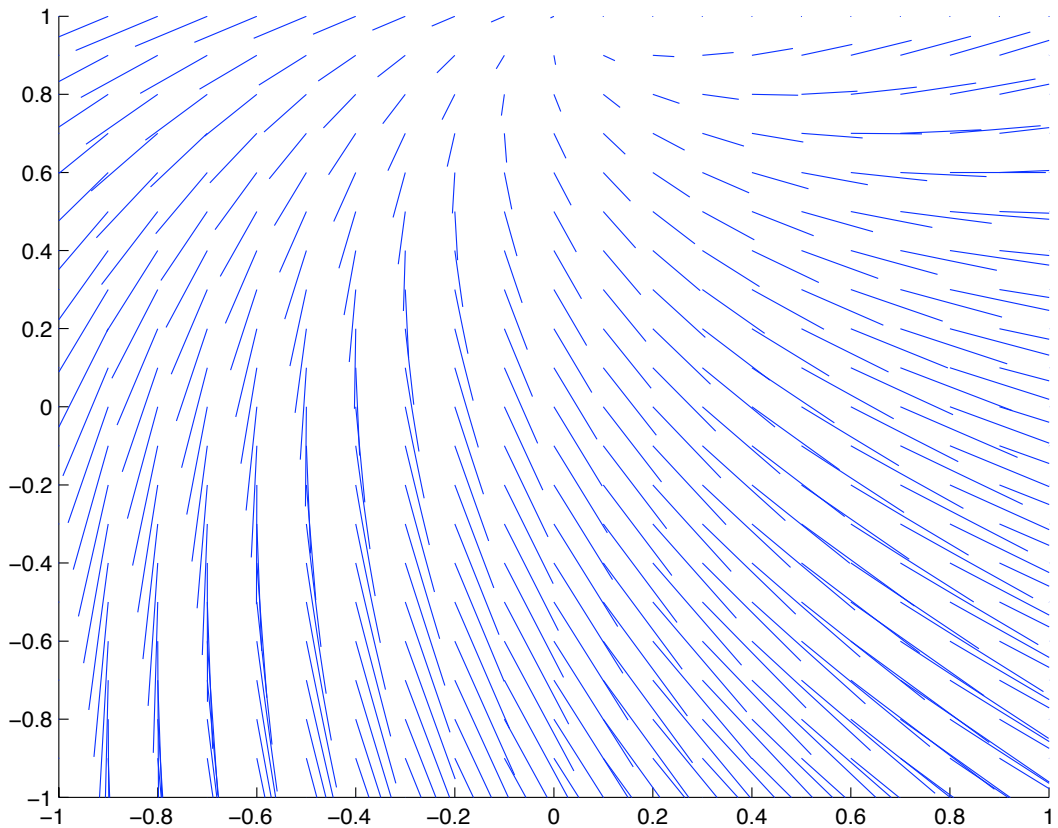


Figure 1.2: This figure is just a simple figure with a width set at 5.5 in. An example of a figure whose size depends on the width of the page is given in Figure A.1 in Section A.1 of Appendix A.

#### 1.4 Math and Equation Example, Where the Heading Is Made so Long That It Extends onto a Second Line

Here is how to use inline math mode to define lambda like this,  $\lambda$ , and how to declare Equations (1.1) and (1.2)

$$I_x(x, y) = \frac{\partial I(x, y)}{\partial x}, \quad (1.1)$$

$$I_y(x, y) = \frac{\partial I(x, y)}{\partial y}. \quad (1.2)$$

Or you can create equation arrays like

$$\alpha = \beta^\gamma \quad (1.3)$$

$$x = \frac{1}{\alpha} \quad (1.4)$$

$$y = \sqrt{\left| \frac{\gamma}{\beta} \right|} \quad (1.5)$$

$$\zeta = x^y. \quad (1.6)$$

The lines in the array can be referenced by saying things like: In Eqn. (1.4) we show a wonderful equation, but it's not nearly as amazing as Eqn. (1.6).

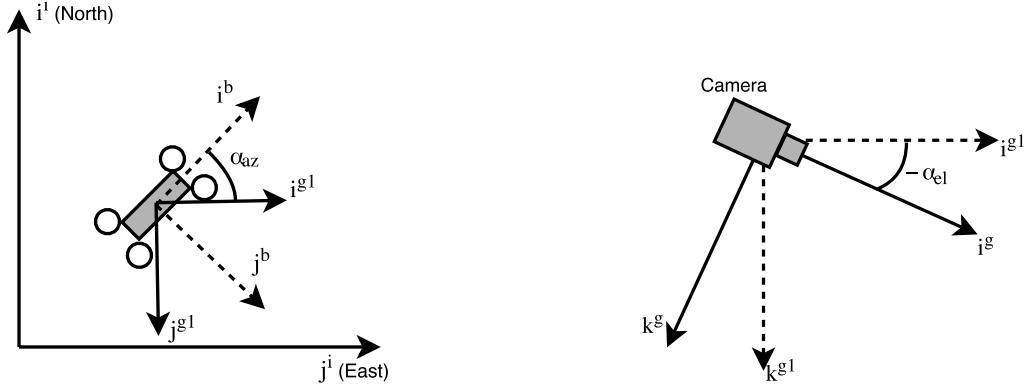
## CHAPTER 2. GIMBAL CONTROL

Gimbal is a widely used device for flying drones with camera because it stabilizes the camera from vibration and movement of the platform. Stabilizing camera is important in order to take high-quality, smooth videos and photos. For this reason, most of high-end commercial drones are equipped with gimbal. For autonomous systems, gimbal becomes more important because it adds maneuverability to the camera to provide with more visual awareness and to keep the object of interest in the camera field of view. There are two ways to keep the object of interest in the camera field of view: First, when we know the relative location of the target to the camera. Second, when we know the target location in image. For many practical applications, it is not feasible to assume that we know the target location in global frame. Thus, image-based gimbal control becomes more practical and realistic way to achieve the goal. In this chapter, we introduce multiple image-based gimbal control schemes.

### 2.1 Angle Commanding Gimbal Control

#### 2.1.1 Coordinate Frame Convention and Projective Camera Geometry

Before giving a detailed explanation of the gimbal control algorithms, it is worth to set up the coordinate frame convention and projective camera geometry. Note that the coordinate frame convention here is following the convention from chapter 13 of [1]. We assume that the origins of gimbal and camera frames are on the same point as the center of mass (COM) of the UAV. This is a reasonable assumption because the distance between camera, gimbal and the UAV COM is negligible compared to the distance between the UAV COM and the target. Also, note that all coordinate frames and the direction of rotation follow the right-hand rule. There are four frames of interests: the body frame of the UAV denoted by  $\mathcal{F}^b = (i^b, j^b, k^b)$ , the gimbal-1 frame denoted by  $\mathcal{F}^{g1} = (i^{g1}, j^{g1}, k^{g1})$ , the gimbal frame denoted by  $\mathcal{F}^g = (i^g, j^g, k^g)$ , and the camera frame



(a) Top view to show the relationship between body frame and gimbal-1 frame (b) Side view to show the relationship between gimbal-1 frame and gimbal frame

Figure 2.1: Frames of interest: body frame, gimbal-1 frame, and gimbal frame

denoted by  $\mathcal{F}^c = (i^c, j^c, k^c)$ . The gimbal-1 frame can be obtained by rotating  $\mathcal{F}^b$  about  $k^b$  axis by  $\alpha_{az}$  which we call the gimbal azimuth angle. The gimbal frame can be obtained by rotating  $\mathcal{F}^{g1}$  about  $j^{g1}$  axis by  $-\alpha_{el}$  which we call the gimbal elevation angle. The negative sign is added because gimbal tilts down where tilting up is positive rotation (See Fig. 2.1). The camera frame is following the same direction as the pixel value grows in image with  $k^c$  axis pointing straight out of the camera sensor. Thus, the rotation from body frame to gimbal-1 frame can be expressed as

$$R_b^{g1}(\alpha_{az}) = \begin{bmatrix} \cos \alpha_{az} & \sin \alpha_{az} & 0 \\ -\sin \alpha_{az} & \cos \alpha_{az} & 0 \\ 0 & 0 & 1 \end{bmatrix}. \quad (2.1)$$

Similarly, the rotation from gimbal-1 frame to gimbal frame can be expressed as

$$R_{g1}^g(-\alpha_{el}) = \begin{bmatrix} \cos(-\alpha_{el}) & 0 & \sin(-\alpha_{el}) \\ 0 & 1 & 0 \\ -\sin(-\alpha_{el}) & 0 & \cos(-\alpha_{el}) \end{bmatrix} = \begin{bmatrix} \cos \alpha_{el} & 0 & -\sin \alpha_{el} \\ 0 & 1 & 0 \\ \sin \alpha_{el} & 0 & \cos \alpha_{el} \end{bmatrix} = R_{g1}^g(\alpha_{el}). \quad (2.2)$$

The last two equations from the equation 2.2 allow to use just the angle between  $i^{g1}$  and  $i^g$  without having to add the negative sign before the angle value. Combining the equations 2.1 and 2.2, we

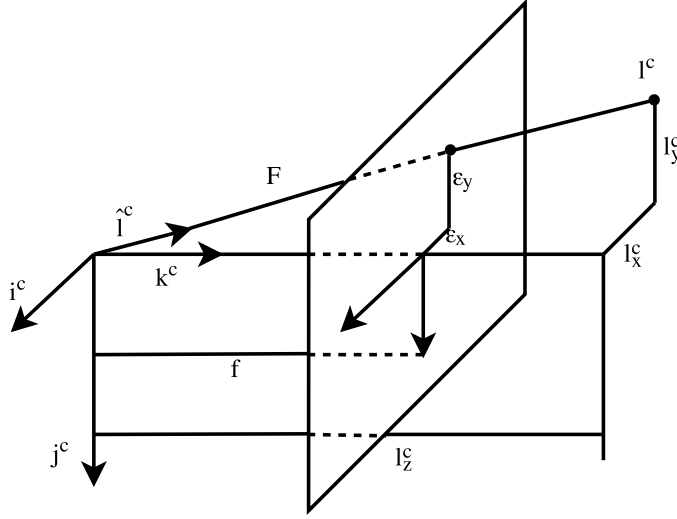


Figure 2.2: Camera frame and visual aid for projective camera model

get the rotation from the body frame  $\mathcal{F}^b$  to gimbal frame  $\mathcal{F}^g$

$$R_b^g(\alpha_{az}, \alpha_{el}) = R_{g1}^g(\alpha_{az})R_b^{g1}(\alpha_{el}) = \begin{bmatrix} \cos \alpha_{el} \cos \alpha_{az} & \cos \alpha_{el} \sin \alpha_{az} & -\sin \alpha_{el} \\ -\sin \alpha_{az} & \cos \alpha_{az} & 0 \\ \sin \alpha_{el} \cos \alpha_{az} & \sin \alpha_{el} \sin \alpha_{az} & \cos \alpha_{el} \end{bmatrix}. \quad (2.3)$$

The camera frame, often referred as optical frame, is following the common computer vision convention:  $i$ -axis grows to the right,  $j$ -axis grows to the bottom and  $k$ -axis grows to the out from the camera optical sensor (See Fig. 2.2). Thus, the rotation from the gimbal frame to the camera frame is fixed once a camera is mounted on a gimbal and is given by

$$R_g^c = \begin{bmatrix} 0 & 1 & 0 \\ 0 & 0 & 1 \\ 1 & 0 & 0 \end{bmatrix}. \quad (2.4)$$

The basic idea of the projective camera model is that the real 3D world is projected onto a 2D image plane that is orthogonal to  $k^c$  axis with distance being the focal length  $f$  from the origin of the optical axis (See Fig. 2.2). Because of this projection, we lose the distance information to the target which has introduced wide research problems in computer vision and estimation area. The focal length of the camera is the distance between optical sensor and lens, and it can be obtained

through camera calibration. Since common camera calibration gives the focal length in the unit of pixel, the camera's field of view angle ( $M$ ) can also be obtained as

$$M = 2 \tan^{-1} \left( \frac{\varepsilon_{max}}{f} \right) \quad (2.5)$$

where  $\varepsilon_{max}$  is the maximum pixel value from the center of the image.

### 2.1.2 Derivation

Let the unit vector from the camera frame origin to the target (ie. the line of sight vector or LOS vector) in the camera frame be defined as

$$\hat{\ell}^c = \frac{1}{L} \begin{pmatrix} \varepsilon_x \\ \varepsilon_y \\ f \end{pmatrix} = \frac{1}{\sqrt{\varepsilon_x^2 + \varepsilon_y^2 + f^2}} \begin{pmatrix} \varepsilon_x \\ \varepsilon_y \\ f \end{pmatrix} = \begin{pmatrix} \hat{\ell}_x^c \\ \hat{\ell}_y^c \\ \hat{\ell}_z^c \end{pmatrix}. \quad (2.6)$$

Angle commanding gimbal control algorithm computes the gimbal azimuth and elevation angles that would make the optical axis align with the unit LOS vector. By transforming the unit LOS vector (2.6) into the body frame, we get the desired optical axis direction as shown below

$$\hat{\ell}^b = R_g^b R_c^g \hat{\ell}^c. \quad (2.7)$$

By equating the equation (2.7) to the unit optical axis vector transformed into the body frame, we can compute the desired azimuth and elevation commands as

$$\hat{\ell}^b = \begin{pmatrix} \hat{\ell}_x^b \\ \hat{\ell}_y^b \\ \hat{\ell}_z^b \end{pmatrix} = R_g^b(\alpha_{az}^d, \alpha_{el}^d) R_c^g \begin{pmatrix} 0 \\ 0 \\ 1 \end{pmatrix} \quad (2.8)$$

$$= \begin{bmatrix} \cos \alpha_{el}^d \cos \alpha_{az}^d & -\sin \alpha_{az}^d & \sin \alpha_{el}^d \cos \alpha_{az}^d \\ \cos \alpha_{el}^d \sin \alpha_{az}^d & \cos \alpha_{az}^d & \sin \alpha_{el}^d \sin \alpha_{az}^d \\ -\sin \alpha_{el}^d & 0 & \cos \alpha_{el}^d \end{bmatrix} \begin{bmatrix} 0 & 0 & 1 \\ 1 & 0 & 0 \\ 0 & 1 & 0 \end{bmatrix} \begin{pmatrix} 0 \\ 0 \\ 1 \end{pmatrix} \quad (2.9)$$

$$= \begin{pmatrix} \cos \alpha_{el}^d \cos \alpha_{az}^d \\ \cos \alpha_{el}^d \sin \alpha_{az}^d \\ -\sin \alpha_{el}^d \end{pmatrix}. \quad (2.10)$$

If we solve for  $\alpha_{az}^d$  and  $\alpha_{el}^d$  as

$$\alpha_{az}^d = \tan^{-1} \left( \frac{\hat{\ell}_y^b}{\hat{\ell}_x^b} \right) \quad (2.11)$$

$$\alpha_{el}^d = -\sin^{-1} \left( \hat{\ell}_z^b \right), \quad (2.12)$$

they become the gimbal commands to place the object of interest at the center of image.

### 2.1.3 Hardware Testing Result

The angle commanding control algorithm has been implemented and tested with simple hardware (see Figure 2.3). The major hardware component includes BaseCam SimpleBGC 32-bit gimbal controller, a webcam, DYS 3-axis GoPro gimbal, and AS5048B magnetic rotary encoder attached to each rotating axis to get the exact gimbal angles. Note that in this hardware experiment, the roll axis of gimbal is always commanded to be zero to pan-tilt camera gimbal. The focal length of camera is known through the camera calibration process and the target pixel location is given by the color detection algorithm implemented using OpenCV [2]. The gimbal control algorithm is keeping the target, a line following ground robot, at the center of the camera field of view (see Figure 2.4. Also, the result video can be found at <https://www.youtube.com/watch?v=OZ0Mg8AoAzk>).

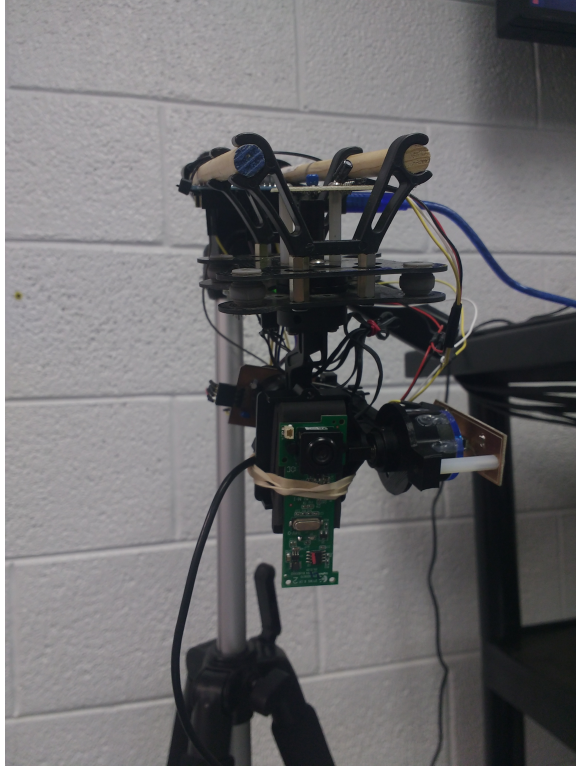


Figure 2.3: Prototype hardware to test gimbal control algorithm

## 2.2 Angular Velocity Commanding Gimbal Control

In the previous section, a relatively simple gimbal control algorithm is presented. One disadvantage of it is that it does not take the camera velocity into consideration. When gimbal is mounted on a stationary platform, the angle commanding controller can perform without any performance degradation. However, if the gimbal is mounted on UAV, taking the camera velocity into account in the controller becomes important. The work in [3] addresses this issue and derives the control algorithm that overcomes the issue. This angular velocity commanding gimbal control algorithm is presented briefly in this section because some of the concepts in this section introduces important background for the next section.

### 2.2.1 Image Jacobian

A full derivation of getting Image Jacobian matrix (often called interaction matrix) can be found in [4]. Here, we only show the final form of Image Jacobian in the process of developing the gimbal control algorithm. Let the camera translational and rotational velocities both expressed

in the camera frame be defined as

$$\mathbf{v}_C = [v_{Cx}, v_{Cy}, v_{Cz}]^\top \quad (2.13)$$

$$\boldsymbol{\omega}_C = [\omega_{Cx}, \omega_{Cy}, \omega_{Cz}]^\top \quad (2.14)$$

$$\boldsymbol{\xi} = [\mathbf{v}_C^\top, \boldsymbol{\omega}_C^\top]^\top. \quad (2.15)$$

In this section,  $[A]$  stands for azimuth frame,  $[E]$  stands for elevation frame, and  $[C]$  stands for camera frame (see Figure 2.5).  $\theta$  indicates the elevation angle and  $\psi$  indicates the azimuth angle. Also, following the convention in Figure 2.2,

$$R_C^E = \begin{bmatrix} 0 & 0 & 1 \\ 1 & 0 & 0 \\ 0 & 1 & 0 \end{bmatrix}. \quad (2.16)$$

Also, let the coordinates of image feature and its velocity can be defined as

$$\mathbf{s} = [u, w]^\top \quad (2.17)$$

and

$$\dot{\mathbf{s}} = [\dot{u}, \dot{w}]^\top. \quad (2.18)$$

Image Jacobian matrix  $L$  shows the relationship between the camera velocity in (2.15) and the image feature velocity in (2.18) and can be expressed as

$$\dot{\mathbf{s}} = L(\mathbf{s}, z, \lambda) \boldsymbol{\xi} \quad (2.19)$$

or more explicitly

$$\begin{bmatrix} \dot{u} \\ \dot{w} \end{bmatrix} = \begin{bmatrix} -\frac{\lambda}{z} & 0 & \frac{u}{z} & \frac{uw}{\lambda} & -\frac{\lambda^2+u^2}{\lambda} & w \\ 0 & -\frac{\lambda}{z} & \frac{w}{z} & \frac{\lambda^2+w^2}{\lambda} & -\frac{uw}{\lambda} & -u \end{bmatrix} \begin{bmatrix} v_{Cx} \\ v_{Cy} \\ v_{Cz} \\ \omega_{Cx} \\ \omega_{Cy} \\ \omega_{Cz} \end{bmatrix} \quad (2.20)$$

where  $z$  is the depth along the optical axis to where the target lies and  $\lambda$  is the focal length. Note that  $\lambda$  is a fixed parameter once the camera is calibrated. The equation (2.20) can be divided into two parts: one for the camera translational velocity and the other for rotational velocity as

$$\dot{\mathbf{s}} = \begin{bmatrix} -\frac{\lambda}{z} & 0 & \frac{u}{z} \\ 0 & -\frac{\lambda}{z} & \frac{w}{z} \end{bmatrix} \mathbf{v}_C + \begin{bmatrix} \frac{uw}{\lambda} & -\frac{\lambda^2+u^2}{\lambda} & w \\ \frac{\lambda^2+w^2}{\lambda} & -\frac{uw}{\lambda} & -u \end{bmatrix} \boldsymbol{\omega}_C \quad (2.21)$$

$$= L_v(u, w, z) \mathbf{v}_C + L_\omega(u, w) \boldsymbol{\omega}_C \quad (2.22)$$

It is worth to note that only the translational part depends on the target depth  $z$ .

## 2.2.2 Feedback Linearization-based Visual Pointing and Tracking

The controller's objective is to drive an image feature to the center of image. The horizontal error can be eliminated by moving two axis gimbal motors attached on azimuth and elevation axis. Moving only the azimuth axis can not compensate for the horizontal error because it only indirectly affects  $E_z$  axis which is often referred as cross-elevation axis *CEL*. Thus, some vertical error is introduced and it needs to be compensated by moving the elevation at next time step. However, the key idea of the controller is that exploiting  $\omega_{Ex}$  term in a clever way we can find the azimuth and elevation commands for the same time step that smoothly compensate for the horizontal error without introducing the vertical error. Let the error in the image plane be

$$e(t) = s(t) - s^{ref} \quad (2.23)$$

where  $s^{ref} = [0, 0]^\top$  to push the image feature to the image center. We would like to derive (2.23) to zeros by controlling  $\omega_{EL} = \omega_{Ey}$  and  $\omega_{AZ} = \frac{\omega_{Ez}}{\cos \theta}$ . Manipulating the equation (2.22) gives

$$L_\omega(u, w)\omega_C = \dot{s} - L_v(u, w, z)\mathbf{v}_C. \quad (2.24)$$

Note that our interest is to find camera angular rate command only and camera translational rate can be measured when UAV is flying independent from the gimbal controller. The null space of the matrix  $L_\omega$  can be parameterized as

$$N(L_\omega) = \{\omega_C = k \begin{bmatrix} u & w & \lambda \end{bmatrix}^\top\} \quad (2.25)$$

and adding (2.25) to (2.24) makes

$$L_\omega(u, w)\omega_C = \dot{s} - L_v(u, w, z)\mathbf{v}_C + L_\omega(u, w)k \begin{bmatrix} u \\ w \\ \lambda \end{bmatrix}. \quad (2.26)$$

This null space means that rotation about the axis connecting the image feature and the origin of optical axis do not change the coordinates of the image feature. The left pseudoinverse of  $L_\omega$  is given by

$$L_\omega^\ddagger = \begin{bmatrix} 0 & \frac{\lambda}{\lambda^2+u^2+w^2} \\ -\frac{\lambda}{\lambda^2+u^2+w^2} & 0 \\ \frac{w}{\lambda^2+u^2+w^2} & -\frac{u}{\lambda^2+u^2+w^2} \end{bmatrix} \quad (2.27)$$

and multiplying both side of (2.26) by (2.27) yields

$$\omega_C = \frac{1}{z(\lambda^2+u^2+w^2)} \begin{bmatrix} \lambda^2 v_y - \lambda v_z w + \lambda \dot{w} z + k u \\ -\lambda^2 v_x + \lambda v_z u - \lambda \dot{u} z + k w \\ -\lambda u v_y + \lambda w v_x - u \dot{w} z + \dot{u} w z + k \lambda \end{bmatrix}. \quad (2.28)$$

If we require  $\dot{s}^{ref}(t) = -\alpha Is(t)$  where  $\alpha$  is a positive value, the actual value of  $s(t)$  is expected to be exponentially stable which means it converges to zero. Thus,

$$\dot{s}^{ref} = \begin{bmatrix} \dot{u}^{ref} \\ \dot{w}^{ref} \end{bmatrix} = -\alpha \begin{bmatrix} 1 & 0 \\ 0 & 1 \end{bmatrix} \begin{bmatrix} u \\ w \end{bmatrix} = \begin{bmatrix} -\alpha u \\ -\alpha w \end{bmatrix}. \quad (2.29)$$

By plugging the equation (2.29) into (2.28), we can compute the desired camera angular rate that guarantees the asymptotic stability for the image error as

$$\omega_C^{ref} = \frac{1}{z(\lambda^2 + u^2 + w^2)} \begin{bmatrix} \lambda^2 v_y - \lambda v_z w - \lambda \alpha w z + k u \\ -\lambda^2 v_x + \lambda v_z u + \lambda \alpha u z + k w \\ -\lambda u v_y + \lambda w v_x + k \lambda \end{bmatrix}. \quad (2.30)$$

This angular rate reference commands expressed in the camera frame must be transformed into the elevation frame in order to make them direct command for each gimbal axis as

$$\omega_E^{ref} = R_C^E \omega_C^{ref} = \begin{bmatrix} \omega_{Ex}^{ref} \\ \omega_{Ey}^{ref} \\ \omega_{Ez}^{ref} \end{bmatrix} \quad (2.31)$$

$$= \frac{1}{z(\lambda^2 + u^2 + w^2)} \begin{bmatrix} -\lambda u v_y + \lambda w v_x + k \lambda \\ \lambda^2 v_y - \lambda v_z w - \lambda \alpha w z + k u \\ -\lambda^2 v_x + \lambda v_z u + \lambda \alpha u z + k w \end{bmatrix}. \quad (2.32)$$

It is questionable that  $\omega_C^{ref}$  has commands for three axis, but there are only two controllable axis, namely  $\omega_{Ey}$  and  $\omega_{Ez}$ . This problem can be solved by using the free parameter  $k$  to come up with two proper motor commands. The key strategy of picking  $k$  is to select the  $k$  value that does not require any change from the current  $\omega_{Ex}$  value as

$$k = u v_y - w v_x + \frac{z(\lambda^2 + u^2 + w^2)}{\lambda} \omega_{Ex} \quad (2.33)$$

which indicates that  $\omega_x$  must be measured from a sensor such as MEMS gyro attached to the camera. Substituting for  $k$  in  $\omega_{Ey}^{ref}$  and  $\omega_{Ez}^{ref}$  from the equation (2.32) with (2.33) gives

$$\omega_{EL}^{ref} = \omega_{Ey}^{ref} = \frac{\lambda^2 v_y - \lambda v_z w - \lambda \alpha w z + u^2 v_y - u w v_x}{z(\lambda^2 + u^2 + w^2)} + \frac{\omega_{Ex} u}{\lambda} \quad (2.34)$$

$$\omega_{CEL}^{ref} = \omega_{Ez}^{ref} = \frac{-\lambda^2 v_x + \lambda v_z u + \lambda \alpha u z + u w v_y - w^2 v_x}{z(\lambda^2 + u^2 + w^2)} + \frac{\omega_{Ex} w}{\lambda}. \quad (2.35)$$

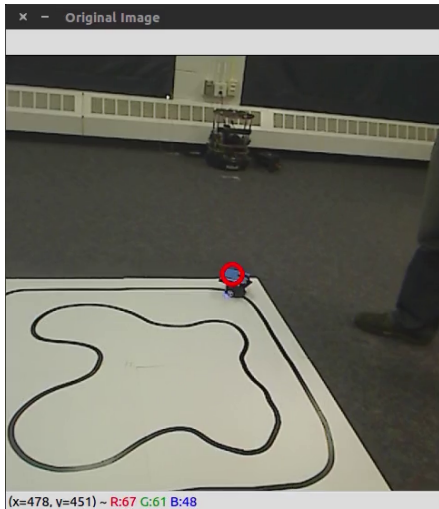
Using the relationship

$$\omega_{AZ} = \frac{1}{\cos \theta} \omega_{CEL}, \quad (2.36)$$

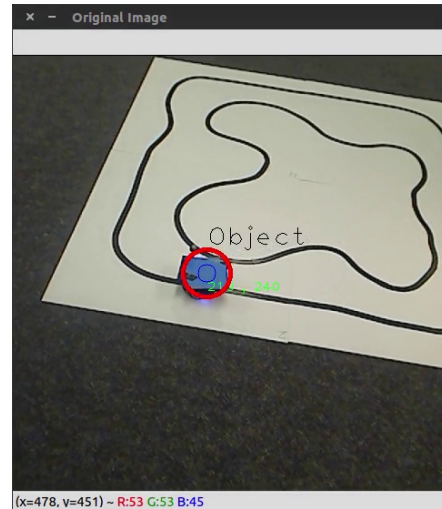
we can compute the desired angular rate on azimuth axis instead of cross-elevation axis as

$$\omega_{AZ}^{ref} = \frac{1}{\cos \theta} \left( \frac{-\lambda^2 v_x + \lambda v_z u + \lambda \alpha u z + u w v_y - w^2 v_x}{z(\lambda^2 + u^2 + w^2)} + \frac{\omega_{Ex} w}{\lambda} \right). \quad (2.37)$$

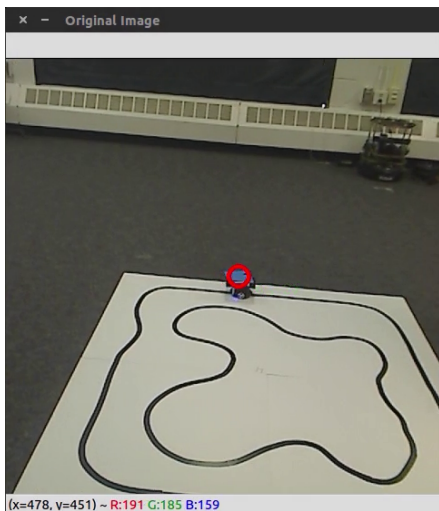
The system block diagram of this controller can be found in Figure 2.6. The controller presents the ideal control scheme for two axis inertially stabilized gimbal system, but it also presents some technical challenges such as estimating the depth to the target and the camera translational velocity.



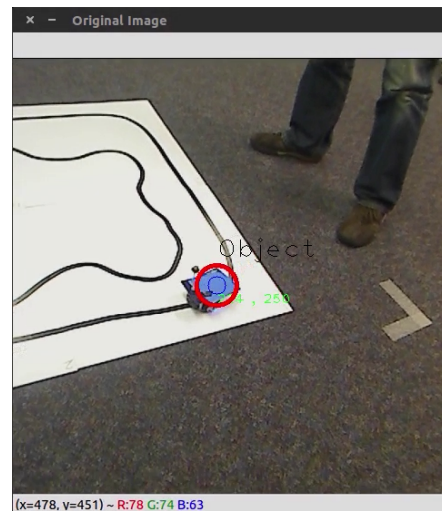
(a) when  $t = 0s$



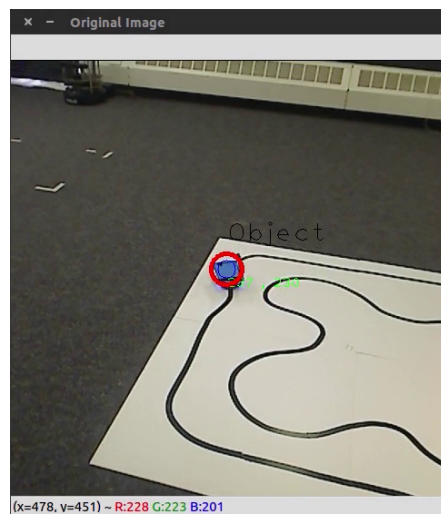
(b) when  $t = 10s$



(c) when  $t = 20s$



(d) when  $t = 30s$



(e) when  $t = 40s$

Figure 2.4: Hardware demonstration. The gimbal control algorithm is keeping the target object at the center of the camera field of view.

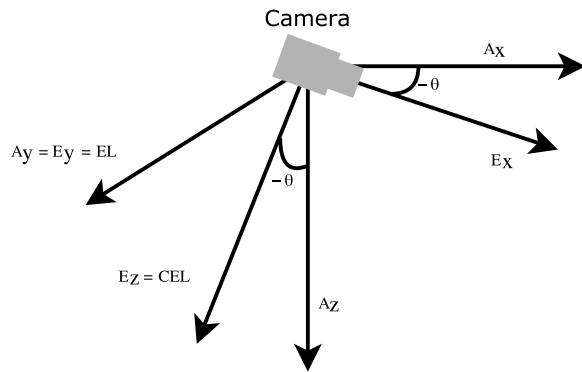


Figure 2.5: Elevation and cross-elevation axis

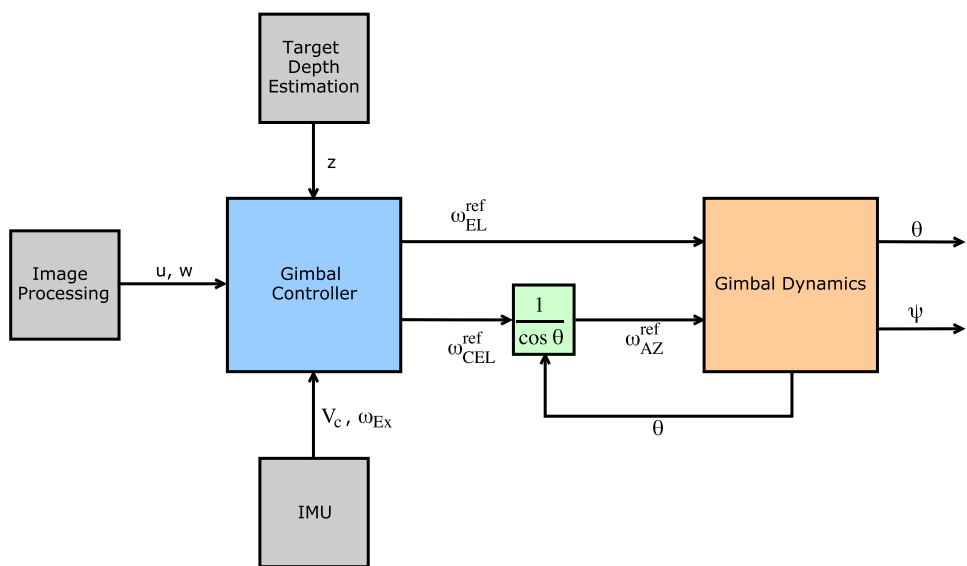


Figure 2.6: Angular velocity commanding gimbal controller block diagram

## CHAPTER 3. UAV CONTROL

### 3.1 UAV visual-servoing controller using projective camera geometry

This section introduces a relatively simple UAV control algorithm based on the projective camera geometry. We assume that the controller receives where target is in normalized image coordinate and camera is rigidly fixed to UAV platform.

#### 3.1.1 Coordinate Frame Convention

Before giving a detailed explanation of the control algorithm, it is worth clarifying our assumptions and the coordinate frames used in this section.

First, an East-North-Up (ENU) coordinate frame is used as opposed to the common North-East-Down (NED) coordinates for UAV in order to match the frame convention used in the `mavros` package in ROS for hardware experiment. Let  $\mathcal{F}^i$  be the inertial frame, which in this case coincides with the ENU frame, and let  $\mathcal{F}^v$  be the vehicle frame that is translated to the UAV center of mass, with the same orientation as  $\mathcal{F}^i$ . Vehicle-1 frame,  $\mathcal{F}^{v1}$  indicates the frame that is only rotated about the  $z$ -axis of  $\mathcal{F}^v$  by  $\psi$ , the heading angle of the multirotor. The rotation matrix from  $\mathcal{F}^v$  to  $\mathcal{F}^{v1}$  can be expressed as  $R_v^{v1}$ . Other involved frames are optical, camera, and body frames expressed as  $\mathcal{F}^o$ ,  $\mathcal{F}^c$ ,  $\mathcal{F}^b$ , respectively.

Second, a flat-earth model is used to properly scale the target position relative to the camera in  $\mathcal{F}^{v1}$  and we have access to the correct altitude information.

Third, the displacement between the center of mass of the UAV and the focal point of camera is ignored since it is negligible compared to the distance between the camera and the target.

Fourth, we rely on GPS position controller on autopilot. The visual-servoing controller in this paper computes the desired multirotor position in order to follow the target and send the position command to the autopilot.

### 3.1.2 Forward and heading motion control

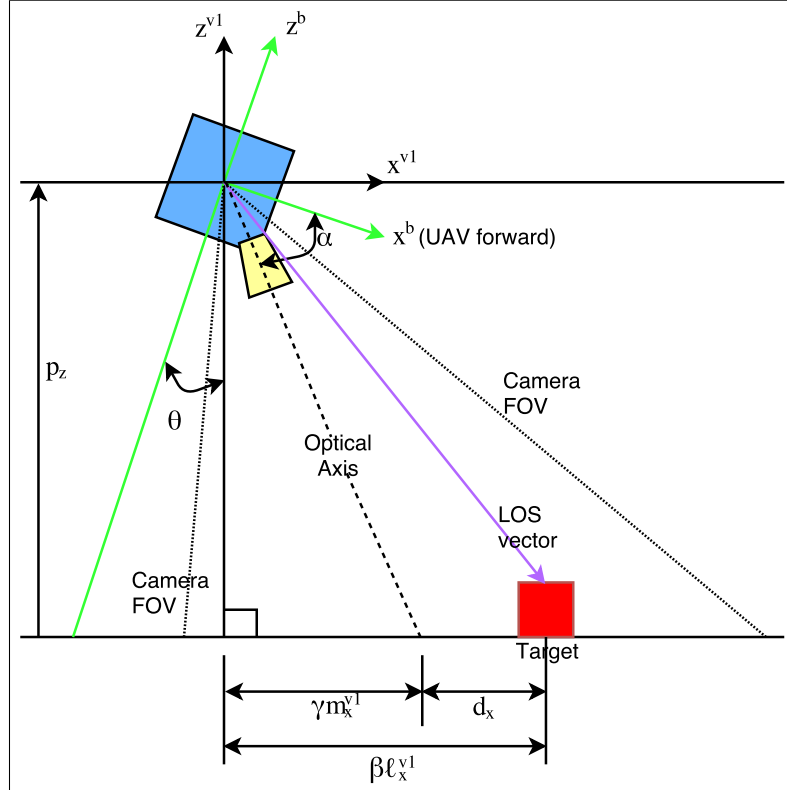


Figure 3.1: Side view of the multirotor.

The first step of the motion control is to transform the line of sight (LOS) vector to the target in  $\mathcal{F}^o$  into  $\mathcal{F}^{v1}$ . Let

$$\ell^o = [\varepsilon_x^o, \varepsilon_y^o, 1]^\top \quad (3.1)$$

where  $\ell^o$  is the normalized line of sight vector in  $\mathcal{F}^o$  and its third element 1 indicates the focal length of the camera in the normalized image. Let also the unit vector along the optical axis in  $\mathcal{F}^o$  be defined as

$$\mathbf{m}^o = [0, 0, 1]^\top. \quad (3.2)$$

By applying sequential transformations to  $\ell^o$  and  $\mathbf{m}^o$ , we get

$$\ell^{v1} = R_b^{v1}(\phi, \theta) R_c^b(\alpha) R_o^c \ell^o = [\ell_x^{v1}, \ell_y^{v1}, \ell_z^{v1}]^\top \quad (3.3)$$

$$\mathbf{m}^{v1} = R_b^{v1}(\phi, \theta) R_c^b(\alpha) R_o^c \mathbf{m}^o = [m_x^{v1}, m_y^{v1}, m_z^{v1}]^\top \quad (3.4)$$

where  $R_c^b$  is a matrix with fixed values depending on how the camera is mounted with respect to  $\mathcal{F}^b$ ,  $R_b^{v1}$  is a matrix requiring the roll and pitch angles of the multirotor. The  $\ell^{v1}$  is the displacement of the target relative to the multirotor and  $\mathbf{m}^{v1}$  is the optical axis in  $\mathcal{F}^{v1}$ . The LOS vector  $\ell^{v1}$  and  $\mathbf{m}^{v1}$  do not have proper scalings due to the unknown depth information to the target in  $\mathcal{F}^o$ , but can be recovered using the altitude of the camera. Let

$$\beta = \frac{p_z}{\ell_z^{v1}} \quad (3.5)$$

$$\gamma = \frac{p_z}{m_z^{v1}} \quad (3.6)$$

where  $p_z$  is the altitude of the multirotor. Then, the desired forward position from the current multirotor position can be computed as

$$d_x = \beta \ell_x^{v1} - \gamma m_x^{v1}. \quad (3.7)$$

This  $d_x$  may be further broken down into east and north components

$$d_n = d_x \sin(\psi) \quad (3.8)$$

$$d_e = d_x \cos(\psi) \quad (3.9)$$

where  $\psi$  is the heading of the multirotor. These north and east components are added to the current multirotor east and north positions, and the sum is sent to the autopilot position controller.

It is more suitable to compensate for a target moving horizontally in the image plane by adjusting the multirotor's heading than through lateral motion. Thus, a yaw rate command  $\omega_z$  can be computed as

$$\omega_z = \eta \ell_y^{v1}, \quad (3.10)$$

where  $\eta > 0$  is a control gain.

## CHAPTER 4. ADVANCED UAV CONTROL

### 4.1 Motivation

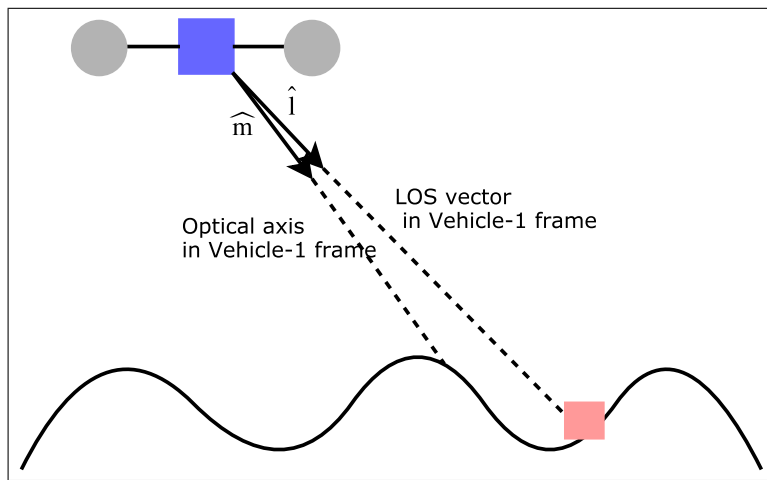


Figure 4.1: Non-flat-earth model example. The unit optical axis vector  $\hat{m}$  and the unit line of sight vector  $\hat{l}$  are key components of the controller presented in this chapter.

The UAV control algorithm introduced in the previous chapter is relatively simple and easy to implement. Anyone with sound understanding of projective camera geometry and frame transformation would not have difficult time to implement the algorithm. However, the controller makes strong assumption that can be unrealistic for some cases. It assumes that the line of sight (LOS) vector to the target and the optical axis lie on the same flat surface which is often called 'flat-earth assumption'. Then, the altitude of multirotor acts as scale factor that had been lost due to the projective camera model to compute how much the UAV has to move forward. An advanced UAV controller presented in this chapter overcomes the flat-earth assumption by working out with the unit LOS vector and unit optical axis vector (see Figure 4.1). Also, the controller does not require the altitude of multirotor to be known because the scale factor does not have to be recovered.

## 4.2 Controller Derivation for Simple UAV dynamics

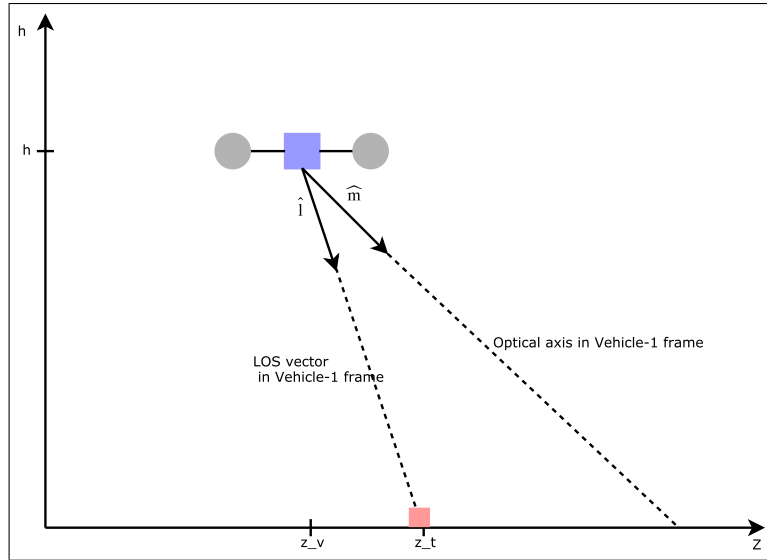


Figure 4.2: Graphical overview of the problem

As a process of developing an advanced control algorithm, we start with a simple vehicle dynamics as

$$\ddot{z}_v = u_1 \quad (4.1)$$

$$\ddot{h} = u_2 \quad (4.2)$$

where  $z_v$  is multirotor's horizontal position and  $h$  is its altitude. A required input to the proposed controller is the unit LOS vector and it is measurable. Let the projection matrix onto the null space

of  $\hat{m}$  be

$$P_{\hat{m}} = (I - \hat{m}\hat{m}^\top) \quad (4.3)$$

$$= \begin{pmatrix} 1 & 0 & 0 \\ 0 & 1 & 0 \\ 0 & 0 & 1 \end{pmatrix} - \begin{pmatrix} m_1 \\ m_2 \\ 0 \end{pmatrix} \begin{pmatrix} m_1 & m_2 & 0 \end{pmatrix} \quad (4.4)$$

$$= \begin{pmatrix} 1 - m_1^2 & -m_1 m_2 & 0 \\ -m_1 m_2 & 1 - m_2^2 & 0 \\ 0 & 0 & 1 \end{pmatrix} \quad (4.5)$$

The objective is to drive the horizontal component of  $P_{\hat{m}}\hat{l}$  to zero. If we let

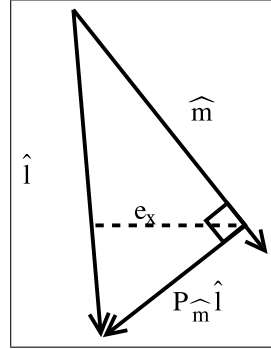


Figure 4.3: Projection onto the null space of the optical axis unit vector

$$\hat{e}_1 = [1 \ 0 \ 0]^\top, \quad (4.6)$$

the horizontal component of  $P_{\hat{m}}\hat{l}$  which is denoted by  $e_x$  can be expressed as

$$e_x = \hat{e}_1^\top P_{\hat{m}}\hat{l}. \quad (4.7)$$

Note that since  $\hat{m}$  is fixed and known and  $\hat{l}$  is measured,  $e_x$  can also be measured. Also, since  $\hat{l}$  can be approximated by differentiating numerically,

$$\dot{e}_x = \hat{e}_1^\top P_{\hat{m}}\dot{\hat{l}} \quad (4.8)$$

is measurable. Meanwhile, the line of sight vector is

$$l = \begin{pmatrix} z_t \\ 0 \\ 0 \end{pmatrix} - \begin{pmatrix} z_v \\ h \\ 0 \end{pmatrix}. \quad (4.9)$$

Differentiating the equation (4.9) once and twice gives

$$\dot{l} = \begin{pmatrix} \dot{z}_t \\ 0 \\ 0 \end{pmatrix} - \begin{pmatrix} \dot{z}_v \\ \dot{h} \\ 0 \end{pmatrix} \quad (4.10)$$

$$\ddot{l} = \begin{pmatrix} \ddot{z}_t \\ 0 \\ 0 \end{pmatrix} - \begin{pmatrix} \ddot{z}_v \\ \ddot{h} \\ 0 \end{pmatrix}. \quad (4.11)$$

Assuming that the acceleration of target is constant and the UAV altitude (ie  $u_2 = 0$ ) is not changing yields

$$\ddot{l} = \begin{pmatrix} -\ddot{z}_v \\ 0 \\ 0 \end{pmatrix} = \begin{pmatrix} -u_1 \\ 0 \\ 0 \end{pmatrix}. \quad (4.12)$$

Thus, combining the equations (4.5), (4.6) and (4.12) results in

$$\hat{e}_1^\top P_{\hat{m}} \ddot{l} = -(1 - m_1^2)u_1. \quad (4.13)$$

Let

$$L = \|l\|, \quad (4.14)$$

the depth between camera and target or the norm of LOS vector which is unknown quantity and this is the reason why the controller is developed around the unit LOS vector

$$\hat{l} = \frac{l}{L}. \quad (4.15)$$

Differentiating the equation (4.15) gives

$$\dot{\hat{l}} = \frac{\dot{l}L - l\dot{L}}{L^2} = \frac{\dot{l}}{L} - \hat{l}\left(\frac{\dot{L}}{L}\right). \quad (4.16)$$

Differentiating again gives

$$\ddot{\hat{l}} = \frac{\ddot{l}L - \dot{l}\dot{L}}{L^2} - \dot{\hat{l}}\left(\frac{\dot{L}}{L}\right) - \hat{l}\left(\frac{\ddot{L}L - \dot{L}^2}{L^2}\right) \quad (4.17)$$

$$= \frac{\ddot{l}}{L} - \left(\frac{\dot{l}}{L}\right)\left(\frac{\dot{L}}{L}\right) - \dot{\hat{l}}\left(\frac{\dot{L}}{L}\right) - \hat{l}\left(\frac{\ddot{L}}{L}\right) + \hat{l}\left(\frac{\dot{L}}{L}\right)^2. \quad (4.18)$$

Plugging in for  $\frac{\dot{l}}{L} = \dot{\hat{l}} + \hat{l}\left(\frac{\dot{L}}{L}\right)$  from equation (4.16) into (4.19) gives

$$\ddot{\hat{l}} = \frac{\ddot{l}}{L} - 2\dot{\hat{l}}\left(\frac{\dot{L}}{L}\right) - \hat{l}\left(\frac{\ddot{L}}{L}\right). \quad (4.19)$$

Differentiating the equation (4.8) and plugging the equation (4.19) for  $\ddot{\hat{l}}$  yields

$$\ddot{e}_x = \hat{e}_1^\top P_{\hat{m}} \ddot{\hat{l}} \quad (4.20)$$

$$= \hat{e}_1^\top P_{\hat{m}} \left( \frac{\ddot{l}}{L} - 2\dot{\hat{l}}\left(\frac{\dot{L}}{L}\right) - \hat{l}\left(\frac{\ddot{L}}{L}\right) \right) \quad (4.21)$$

$$= \frac{1}{L}(\hat{e}_1^\top P_{\hat{m}} \ddot{l}) + \frac{\dot{L}}{L}(-2\hat{e}_1^\top P_{\hat{m}} \dot{\hat{l}}) + \frac{\ddot{L}}{L}(-\hat{e}_1^\top P_{\hat{m}} \hat{l}). \quad (4.22)$$

Substituting (4.13) for  $\hat{e}_1^\top P_{\hat{m}} \ddot{l}$  results in

$$\ddot{e}_x = -\frac{1}{L}(1 - m_1^2)u_1 + \frac{\dot{L}}{L}(-2\hat{e}_1^\top P_{\hat{m}} \dot{\hat{l}}) + \frac{\ddot{L}}{L}(-\hat{e}_1^\top P_{\hat{m}} \hat{l}) \quad (4.23)$$

$$= -\beta_1 \phi_1 u_1 + \beta_2 \phi_2 + \beta_3 \phi_3 \quad (4.24)$$

where

$$\beta_1 = \frac{1}{L}, \beta_2 = \frac{\dot{L}}{L}, \beta_3 = \frac{\ddot{L}}{L} \quad (4.25)$$

and

$$\phi_1 = 1 - m_1^2, \phi_2 = -2\hat{e}_1^\top P_{\hat{m}} \dot{\hat{l}}, \phi_3 = -\hat{e}_1^\top P_{\hat{m}} \hat{l}. \quad (4.26)$$

Note that  $\frac{1}{L}$ ,  $\frac{\dot{L}}{L}$ , and  $\frac{\ddot{L}}{L}$  are unknown and not measurable whereas the rest of above equation is either known or measurable.

In order to drive  $e_x$  to zero, let's define

$$s = \dot{e}_x + k e_x \quad (4.27)$$

where  $k > 0$ . The reason why the equation (4.27) is selected is because when  $s \rightarrow 0$ ,

$$\dot{e}_x = -k e_x \quad (4.28)$$

which makes  $e_x$  asymptotically stable. Thus, if we can find the control input  $u_1$  that makes  $s \rightarrow 0$ ,  $e_x$  would converge to zero. Differentiating the equation (4.27) and substituting (4.24) for  $\ddot{e}_x$  yields

$$\dot{s} = \ddot{e}_x + k \dot{e}_x \quad (4.29)$$

$$= -\beta_1 \phi_1 u_1 + \beta_2 \phi_2 + \beta_3 \phi_3 + k \dot{e}_x. \quad (4.30)$$

If we know  $\beta_1$ ,  $\beta_2$ , and  $\beta_3$ , the ideal control input would be

$$u_1 = \frac{1}{\beta_1 \phi_1} (\beta_2 \phi_2 + \beta_3 \phi_3 + k \dot{e}_x + \alpha s) \quad (4.31)$$

where  $\alpha > 0$ . Then,

$$\dot{s} = -\alpha s \quad (4.32)$$

which makes  $s$  asymptotically stable. However, since we don't know  $\beta_1$ ,  $\beta_2$ , and  $\beta_3$ , the actual control input would be

$$u_1 = \frac{1}{\hat{\beta}_1 \phi_1} (\hat{\beta}_2 \phi_2 + \hat{\beta}_3 \phi_3 + k \dot{e}_x + \alpha s) \quad (4.33)$$

where  $\hat{\beta}_1$ ,  $\hat{\beta}_2$ , and  $\hat{\beta}_3$  are the estimates of  $\beta_1$ ,  $\beta_2$ , and  $\beta_3$  respectively. Manipulating (4.30) and plugging the actual control (4.33) in (4.34) results in

$$\dot{s} = -\beta_1 \phi_1 u_1 + \hat{\beta}_1 \phi_1 u_1 - \hat{\beta}_1 \phi_1 u_1 + \beta_2 \phi_2 + \beta_3 \phi_3 + k \dot{e}_x \quad (4.34)$$

$$= -(\beta_1 - \hat{\beta}_1) \phi_1 u_1 + (\beta_2 - \hat{\beta}_2) \phi_2 + (\beta_3 - \hat{\beta}_3) \phi_3 - \alpha s \quad (4.35)$$

$$= -\tilde{\beta}_1 \phi_1 u_1 + \tilde{\beta}_2 \phi_2 + \tilde{\beta}_3 \phi_3 - \alpha s \quad (4.36)$$

$$= \tilde{B}^\top \Phi - \alpha s \quad (4.37)$$

where

$$B = \begin{pmatrix} \beta_1 \\ \beta_2 \\ \beta_3 \end{pmatrix}, \hat{B} = \begin{pmatrix} \hat{\beta}_1 \\ \hat{\beta}_2 \\ \hat{\beta}_3 \end{pmatrix}, \tilde{B} = B - \hat{B}, \Phi = \begin{pmatrix} -\phi_1 u_1 \\ \phi_2 \\ \phi_3 \end{pmatrix}. \quad (4.38)$$

In order to show that  $s$  in (4.27) is asymptotically stable and the estimates  $\hat{\beta}_1$ ,  $\hat{\beta}_2$ , and  $\hat{\beta}_3$  are converging to their true values  $\beta_1$ ,  $\beta_2$ , and  $\beta_3$ , a Lyapunov equation can be set as

$$V = \frac{1}{2} s^2 + \frac{1}{2} \tilde{B}^\top \Gamma^{-1} \tilde{B}. \quad (4.39)$$

Then, combining (4.39) with (4.37) results in

$$\dot{V} = s \dot{s} + \tilde{B}^\top \Gamma^{-1} \dot{\tilde{B}} \quad (4.40)$$

$$= s(\tilde{B}^\top \Phi - \alpha s) + \tilde{B}^\top \Gamma^{-1} \tilde{B} \quad (4.41)$$

$$= -\alpha s^2 + \tilde{B}^\top (s\Phi + \Gamma^{-1} \dot{\tilde{B}}). \quad (4.42)$$

Assuming  $B$  is roughly constant or slowly varying (ie  $\dot{B} = 0$ ), the equation (4.42) becomes

$$\dot{V} = -\alpha s^2 + \tilde{B}^\top (s\Phi - \Gamma^{-1} \dot{\tilde{B}}). \quad (4.43)$$

Finally, by choosing  $\dot{\tilde{B}} = s\Gamma\Phi$ ,

$$\dot{V} = -\alpha s^2 \quad (4.44)$$

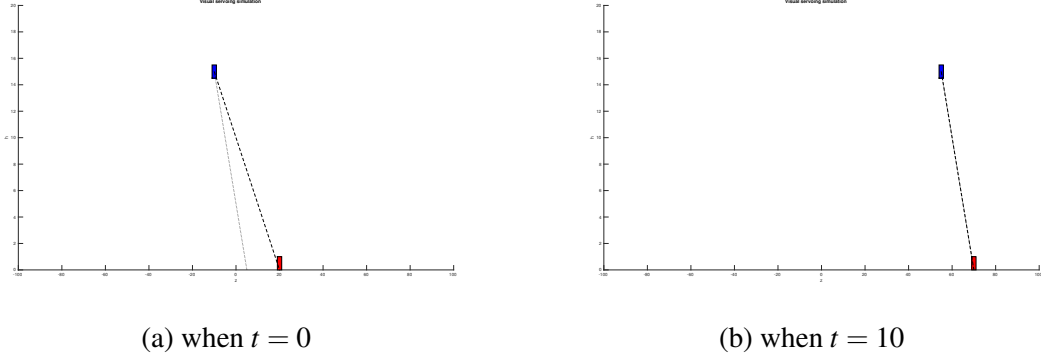


Figure 4.4: Simple UAV dynamics visual servoing Simulink simulation. The blue square is flying UAV at constant altitude and the red square is a target on the ground moving at  $5m/s$

which proves that  $s$  is asymptotically stable. Thus, the original objective of stabilizing  $e_x$  is achieved. This control scheme is simulated in Simulink and the result shows that the above controller is valid (See Figure 4.4 and 4.5).

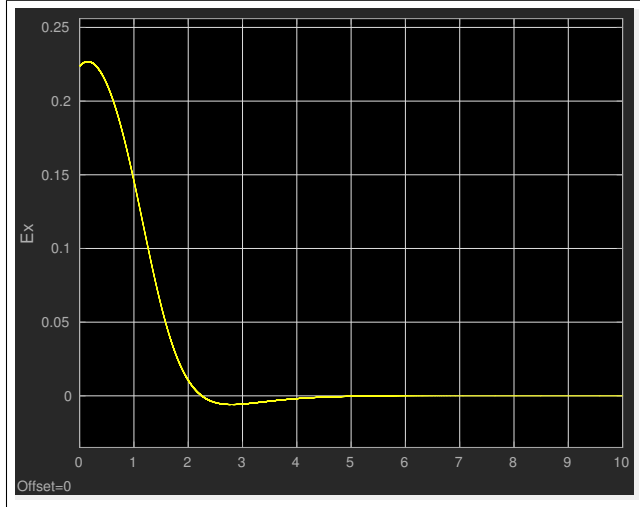


Figure 4.5: The horizontal error between the unit LOS vector and the unit optical axis vector converges to zero.

## REFERENCES

- [1] R. W. Beard and T. W. McLain, *Small unmanned aircraft: Theory and practice*. Princeton university press, 2012. 4
- [2] Itseez, “Open source computer vision library,” <https://github.com/itseez/opencv>, 2015. 8
- [3] Z. Hurak and M. Rezac, “Image-based pointing and tracking for inertially stabilized airborne camera platform,” *IEEE Transactions on Control Systems Technology*, vol. 20, no. 5, pp. 1146–1159, 2012. 9
- [4] M. W. Spong, S. Hutchinson, and M. Vidyasagar, *Robot modeling and control*. Wiley New York, 2006, vol. 3. 9

## APPENDIX A. MAKING A FIGURE WITH WIDTH BASED ON PAGE SIZE

### A.1 Width Based on Page Size Figure Example

Here's an example of a figure whose width depends on the width of the page. You can see it as Figure A.1. This also shows another citation [?].

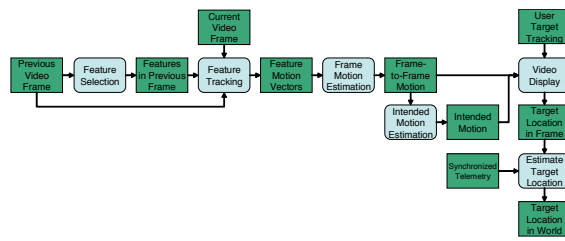


Figure A.1: This is an example of a figure whose width will be 45% of the width of the page. If you'd like to see a figure with a fixed width then you can see it as Figure 1.2 in Section 1.3 of Chapter 1.

## **APPENDIX B. FORMATTING GUIDELINES FOR THESIS**

This appendix outlines the required formatting for theses and dissertations. While the L<sup>A</sup>T<sub>E</sub>X template takes care of most of these automatically, it is the student's responsibility to ensure that all formatting requirements are incorporated in the document.

### **B.1 Font**

Times New Roman 12 pt. throughout text and 10 or 11 point for tables and figures.

### **B.2 Margins**

- Preliminary Pages (Title page, Abstract page(s), Acknowledgment page, Table of Contents, List of Figures, List of Tables): 1 inch on all sides
- Body Pages, beginning with Introduction: 1 inch on all sides
- Chapter title pages, Appendix title page, Reference title page: 2 inches at top, 1 inch at bottom and sides

### **B.3 Printing**

- Single-sided: Title page, Abstract page(s), Acknowledgment page
- Two-sided: Table of Contents, List of Figures, List of Tables, Body, Appendix, References

Note: Table of Contents, List of Figures, List of Tables, Chapter title pages, References and Appendix pages must begin on the front side of a page.

### **B.4 Page Numbering**

- Page numbers are centered at the bottom of the page.

- Counting begins with the Title page; however, back pages are not counted until the Table of Contents.
- Page numbers do not appear on the page until the Table of Contents (v).
- Use Roman Numerals (v, vi, vii, ...) for the Table of Contents page and the pages thereafter until Chapter 1.
- Use Arabic numbers (1, 2, 3 ...) beginning with Chapter 1.
- Be sure numbers appear on all blank back pages once numbering begins.

## B.5 Spacing

- Double-space text of body.
- Single-space abstract, captions, quotes, long chapter titles, headings, and subheadings.
- Table of Contents, List of Figures, List of Tables, and References can be single-spaced or double spaced.
- Double-space three times after chapter titles (48 pts).
- Double-space twice before subheadings (24 pts).
- Double-space once after subheadings (0 pts).
- Double-space once between two subheadings (0 pts).
- Double-space twice before and after figures (24 pts).
- Double-space twice before and after tables (24 pts).
- Double-space once before and after equations (0 pts).
- Do not leave a single line of text, a single-line equation, or a subheading alone on the top (widow) or bottom (orphan) of a page.
- Do not leave more than about 5 lines of white space remaining on a page unless its the end of a chapter.

## B.6 Figures

- Figures are normally diagrams, graphs, maps, or charts.
- Center figures on the page.
- Center captions below the figure. If two lines are needed, the caption should be left justified at margin.
- A figure should be placed after the paragraph of reference. If it will not fit on the same page, continue the text and place the figure on the next page.

## B.7 Tables

- Tables contain numerical or statistical information.
- Center tables on the page.
- Center captions above the table. If more than one line is needed, center the lines in an inverted pyramid:

Table 6.3 Comparison of roll rotation plots when node was displaced, and an X-direction off-axis force was applied.

- If placed in the landscape position, the top of the table should be on the left side of the page, with the caption above the table. The page number is placed in the standard location.